Enhancing the Visualization of the Microvasculature of Extrahepatic Bile Ducts Obtained from Confocal Microscopy Images

Lizeth A.C Beltran*, Jorge Luiz dos Santos[†], Carolina Uribe Cruz[‡], Carla M.D.S Freitas*
*Institute of Informatics
Federal University of Rio Grande do Sul UFRGS, Porto Alegre, Brazil
[†]Centro de Investigação em Ciências da Saúde, Universidade da Beira Interior, Portugal
[‡]Laboratório Experimental de Hepatologia e Gastroenterologia, Porto Alegre, Brazil
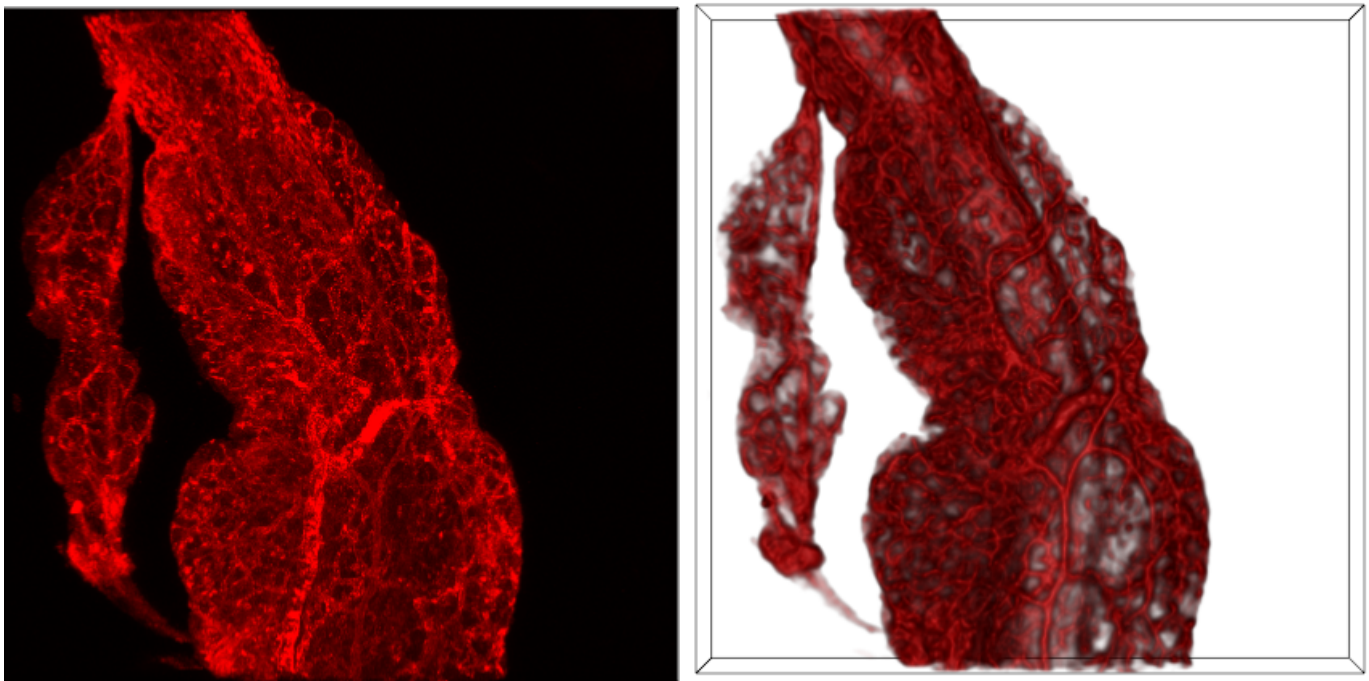{lacbeltran, carla}@inf.ufrgs.br

Fig. 1. Peribiliary Vascular Plexus of an extrahepatic mouse bile duct. Left: 3D visualization of the original confocal dataset. Right: Resulting volume after relevant features enhancement.

Abstract—Confocal microscopy is an important tool for visualizing 3D datasets of fluorescent specimens, and has been used to investigate the structure of biological specimens. However, such images are affected by the noise introduced during the specimen preparation and image acquisition processes. Anisotropic diffusion is a non-linear filter that can significantly improve image quality while removing noise without blurring edges. This study investigates the application of anisotropic diffusion in confocal microscopy images by exploring different models for parameters' estimation. Our data consists of several slices of extrahepatic bile ducts containing a network of small vessels named Peribiliary Vascular Plexus (PVP), which are affected by several sources of noise. Experimental results show that anisotropic diffusion improved the volumetric visualization of the PVP. We validated the results using MSE and PSNR quantitative approaches and qualitative description by an expert user.

Keywords-Anisotropic diffusion; Image processing; Confocal microscopic images; Volumetric Visualization.

I. INTRODUCTION

Bile ducts are tubular structures that carry bile from the liver to the gallbladder and duodenum. Bile ducts are classified as intra- and extrahepatic depending on their position in relation to the liver. [1]. Studying the anatomy of these structures is a hot topic in hepatology research [2]–[5]. In particular, microscopic visualization of bile ducts can provide additional information for detection of morphological changes arising

from biliary diseases. Confocal microscopy enables the acquisition of three dimensional image datasets. In recent years, this technique has been used in medical studies for investigating the micro-anatomical structure of extrahepatic bile ducts [5].

However, there are some challenges associated to confocal imaging. The first challenge is about the image post-processing. Although microscopes provide proprietary software for exploring the datasets, there is still a lack of post-processing techniques to show more details about specific structures of interest. Another challenge is associated to the kind of specimen. Confocal microscopy provides a useful tool to study 3D structure of transparent specimens, because in this case the light can pass through it with minimal scattering [6]. However, bile ducts are nontransparent, thus making necessary the design of specific clearing procedures and staining methods before the image acquisition. Consequently, the images are affected by the noise introduced during the specimen preparation process [7]. In addition to the noise associated to the specimen preparation, the Signal-to-Noise-Ratio (SNR) of the slices of the stack obtained using confocal microscopes is reduced with increasing depth [8]. Hence, the quality of the contrast decreases with increasing depth.

Our work aims at enhancing the quality of images of bile ducts and associated vessels, both obtained by confocal microscopy. In this context, image processing techniques are essential to remove noise and enhance the acquired images. In other kinds of medical images, anisotropic diffusion offers an elegant solution for image enhancement [9]–[12]. We propose the use of anisotropic diffusion to enhance the confocal images, and volumetric visualization techniques to create projections of the bile duct samples in a 3D space so the experts can examine the microvasculature distribution and interact with the bile ducts. Fig. 1 illustrates some results obtained with our approach, showing the volume rendering of the original dataset (left) and the resulting volume after the anisotropic diffusion (right). The network of vessels surrounding the bile duct can be clearly observed. These vessels supply blood to the biliary structures and are called peribiliary vascular plexus (PVP) [13]. The microscopic visualization of PVP is essential to analyze the interrelationship between a bile duct and its vascular plexus, in order to understand the development of biliary diseases associated with vascular disorders.

Contributions: The main contribution of this paper is the enhancement of the volumetric visualization of the PVP obtained from confocal microscopy images. We explore two models to estimate appropriate parameters for the anisotropic diffusion equation used to improve the original volume. As results, we enhance details that are hardly visualized in the original data. Moreover, using interactive manipulation like rotation and zooming operations on the resulting volumetric visualization, the hepatologists can have different views of the microvasculature.

The rest of this paper is organized as follows. Next section briefly discusses the noise present in confocal microscopy images and introduces the classical anisotropic diffusion equation. In Section III, we scrutinize the related works in the field of confocal microscopy images and the estimation of parameters for the anisotropic diffusion equation. Section IV gives details about the bile duct preparation and image acquisition. In Section V we explore two existing models to calculate the k parameter for the anisotropic diffusion equation. The results of our experiments are described in Section VI, and in Section VII we discuss our findings and draw final comments.

II. BACKGROUND

In recent years there has been an explosion in the popularity of confocal microscopy [14], more specifically in cell biology applications using fixed and living cells and tissues. Confocal microscopy data have their own characteristics, which differ from other biomedical data [15]. We describe some operating principles of confocal microscopes to understand the advantages and disadvantages of this technique, which affect directly the data that is being processed. Since, anisotropic diffusion was used to reduce the noise and enhance details of the bile duct images, we also present the basic principles of anisotropic diffusion filtering.

A. Confocal Microscopy Images

In confocal miroscopy the images are acquired point-by-point, using lasers and the principle of fluorescence. Fluorescence is the property of some atoms and molecules to absorb light at a particular wavelength and to subsequently emit light of a longer wavelength after a brief interval [16]. The biological samples can be labeled with several appropriate fluorescent antibodies during the staining process, which allows to mark different tissues or cells. The characteristics of a confocal microscope offer several advantages over conventional optical microscopy such as: the ability of removing out-of-focus light [17], the capability of controlling the depth of field and the capability of collecting several aligned images of the same sample. However, confocal images are normally affected by several artifacts and noise sources:

- Low signal-to-noise ratio: confocal images have a strong decrease in the signal-to-noise ratio over the slices depth [8].
- Diversity of density values: the physical meaning of density values is not limited to image subjects [18]. Confocal images have an inhomogeneous density inherent to the fluorescent staining process [7].
- Visual occluders: structures irrelevant to the analysis may also be labeled through the fluorescent staining process, resulting in visual occluders that obscure the structures to be visualized [19].
- Subtle boundaries: meaningful boundaries may be only subtly presented in the confocal data [19].

Confocal microscopes use proprietary formats. We use datasets acquired by a Leica confocal microscope. These kind of microscopes produce datasets in a format named *LIF* (Leica Image File Format). This specific format encodes the information about the images and the microscope configuration used during acquisition. The information regarding the process of image acquisition is important for further interpretation of the

obtained data by the hepatologist. However, the downside of proprietary formats is that they need proprietary software to decode the stored images [17].

B. Anisotropic Diffusion Filtering

Anisotropic diffusion was introduced by Perona and Malik [20], and has been used as an effective approach in image processing and computer vision for noise removal, edge detection and image restoration [9] [10] The main idea behind this approach is that smoothing should be low on relevant edges and stronger in regions dominated by noise [21]. In the classical formulation [20], the anisotropic diffusion equation is given by the following PDE:

$$\frac{\partial I}{\partial t} = \nabla \cdot c(\nabla I)\nabla I \qquad (1)$$

where t is the time parameter, ∇I is the gradient of the image at time t and c is the diffusivity. The diffusivity can be expressed as a decreasing function of the image gradient magnitude, such as:

$$c(x,t) = e^{-\frac{\nabla I^2}{k}}, c(x,t) = \frac{k^2}{k^2 + \nabla I^2} \qquad (2)$$

where k is the gradient magnitude threshold parameter that controls the rate of the diffusion and serves as a soft threshold between the image gradients that are attributed to noise and those attributed to edges [22]. The great success of the Perona and Malik's model can be mainly attributed to its excellent performance in edge preservation and noise removal [23]. However, the estimation of the parameters for the anisotropic diffusion equation is not an easy task. In this work we explore two models to estimate the k parameter in confocal images (Section V).

III. Related Work

A. Confocal Microscopy Imaging

Related work on confocal microscopy are mostly devoted to biological studies with small structures such as cells. Examples include neurobiology research using animal models such as Drosophila and Zebrafish [15], microtubule spindles during mitosis [24], profiling gene expression of cells [25]–[27], screening phenotypic data and reconstructing the morphology of neurons [28]–[30].

In our research, differently from those previous studies, we analyze a macro structure (the bile duct). Since cells are thinner than bile ducts, this poses a challenge associated to the data because the noisy sources cited in Section II-A affect the image quality in thick specimens to a greater extent than thinner specimens such as cells.

Regarding the use of confocal microscopy to study bile ducts, DiPaola et al. [5] identified networks of glands residing within the bile duct walls. These structures were identified by the visual exploration of the serial sections using the microscope's proprietary software. However, proprietary software has limited possibilities for enhancing the images. Hammad et al. [3] and Vartak et al. [4] used confocal microscopy to

visualize intrahepatic bile ducts that are much smaller than the extrahepatic bile ducts we work on.

B. Image Enhancement in Confocal Images

Usually, the proprietary software that comes with confocal microscopes allows simple contrast enhancement of 2D images. However, image filtering techniques are important when the relevant information is noisy. Median filter is a traditional filter used for noise reduction in confocal images. Parazza et al. [31] used a 3D median filter for noise reduction in confocal microscopy images from cell nuclei. A median filter was also used for noise reduction in images from rat brain [32] In another work, Paul et al. [33] used median filtering to estimate the global noise variance in images from cells. Araujo et al. [34] propose the use of blurring filter, histogram equalization and arithmetic operations to enhance cells from animal nervous system. However, traditional filters, such as the median filter, do not provide significant results to enhance details in our images. That is because they are linear filters performing in all the data, and do not discriminate the important structures we need to improve.

C. Estimating Parameters for the Anisotropic Diffusion Equation

Previous works on anisotropic diffusion indicate that the diffusion process can be improved with the proper choice of parameters of the anisotropic diffusion equation [35] [22]. According to Formaggia et al. [21], the anisotropic filter must be tuned for specific applications in terms of k and t. This implicates that empirical evaluation of the effects of the filter is necessary.

For the estimation of the k parameter, Perona and Malik [20] proposed the use of a noise estimator. This consists in a histogram of the absolute values of the gradient throughout the image and the k is computed as the 90% of its integral. On the other hand, Voci et al. [35] used a morphological approach to estimate k. Several papers discuss aspects for optimizing the anisotropic diffusion. However, none of those proposals are applied to confocal microscopy images.

IV. Image Acquisition

BALB/c mice of 5- and 7-postnatal days were euthanized by overdose of isoflurane and the extrahepatic bile ducts were isolated. The ducts were fixed with Fixer Dent's, rehydrated in decreasing concentrations of MeOH and washed with PBS/BSA/Triton. The preparation methods of bile ducts and related PVP included a technique, developed at the Cincinnati Children's Hospital [5], which is innovative in relation to the mounting of the histologic sample for in situ staining in order to preserve the anatomic structures. This image acquisition was conducted at Hospital de Clinicas de Porto Alegre (HCPA-Brazil). After that, the histologic specimens were labeled with primary antibody: PECAM-1 and CK19 (1:150 Abcam. USA) and secondary antibody Alexa Fluor 647 and 488, respectively (1:150 Abcam. USA). An example of a mouse bile duct after the specimen preparation is shown in Fig. 2.

The handling, caring, and processing of the animals were carried out according to regulations approved by local ethics committee at HCPA (protocol number 11-0190) and complied with the National Guidelines on Animal Care.
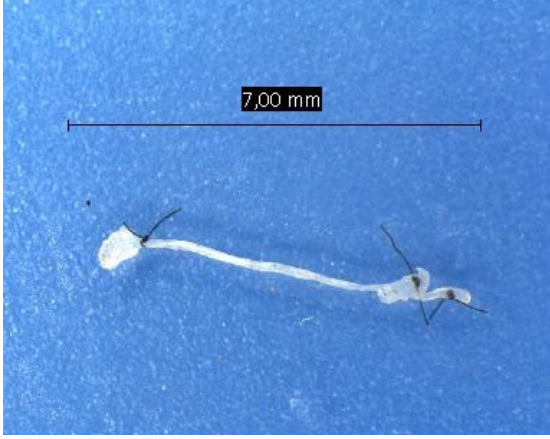

Fig. 2. An extrahepatic mouse bile duct after the clearing and staining process.

Images of all samples were obtained using the confocal microscopy Leica TCS SP5. The resulting datasets had images of 512 x 512 pixels, and the stack was composed by a variable number of slices. Then, the datasets have dimensions *X, Y* and *Z*, where *X* and *Y* are the size of each slice in pixes, and *Z* is the number of slices. Table I illustrates the information about the datasets obtained for each bile duct. The number of slices varies depending on the bile duct size and the microscope settings.

The dataset consists of images with two fluorescence channels. The first one (red channel) represents the PVP stained with PECAM-1, and the second one (green channel) represents the biliary structure stained with CK19. We extracted the red channel because this channel contains the relevant structures that are our focus in this work.

V. ESTIMATING GRADIENT THRESHOLD IN THE CONFOCAL IMAGES DATASET

Anisotropic diffusion only affects parts where the gradient value is below a certain threshold. Therefore, the estimation of this parameter plays an important role in the anisotropic diffusion process. Methods for estimating a suitable value for the *k* parameter are useful in cases in which we have no idea about an appropriate value of the diffusion coefficient and

TABLE I
SIZE OF ACQUIRED DATASETS FROM EXTRAHEPATIC MICE BILE DUCTS.

Dataset Id	Image size (pixels)	# Slices
mouse1-day5	512x512	85
mouse2-day5	512x512	102
mouse3-day5	512x512	116
mouse2-day7	512x512	140
mouse3-day7	512x512	100
mouse4-day7	512x512	117

we would like to perform noise reduction with low loss of details [35]. We compared the two approaches described in related works (Section III-C) to explore the *k* estimation in our images: the first model proposed by Perona and Malik [20] and a second model, proposed by Voci et al. [35]. Then, we use these *k* values as input parameter to calculate the anisotropic diffusion.

A. Estimation of the k parameter using Perona and Malik's model.

The model for the *k* estimation proposed by Perona and Malik [20] is based on a noise estimator using the histogram of the gradient. This noise estimator consists in calculating the histogram of the absolute values of the gradient for every image, and the *k* parameter value is equal to the 90% value of its integral [20].

Fig. 3 shows an example of a slice extracted from our datasets, the gradient histogram calculated for this image and the anisotropic filtering result.

B. Estimation of the k parameter using Voci et al. model.

The model for the *k* estimation proposed by Voci et al. [35] is based on mathematical morphology. The idea of using a morphological approach derives from the fact that morphology can be used for an estimation of noise intensity in the image. Their model is based on opening and closing operations from mathematical morphology. The *k* is given by the following equation:

$$k = \sum_{i,j \in I} \frac{(I(i,j) \circ st)}{(r.c)} - \sum_{i,j \in I} \frac{(I(i,j) \bullet st)}{(r.c)} \quad (3)$$

where $I(i,j)$ refers to the image consisting of r rows and c columns, a structuring element st (we use a st with size 5x5), and the symbols $\circ$ and $\bullet$ represent the opening and closing operations, respectively.

Fig. 4 compares the anisotropic diffusion results using the two different models presented in Section V-A and Section V-B. As can be observed, the results show very similar filtered images using the two models.

VI. PRELIMINARY EXPERIMENTAL RESULTS

The two models for estimating the *k* parameter were implemented in Python. We used the Visualization Toolkit (VTK) [36] to render the confocal datasets. The VTK class (*vtkLIFReader*) was used to load the confocal dataset codified in the LIF format. This class was developed by Kankaanpää et al. [37], and it can be freely used for academic research [38].

Using the models presented in Sections V-A and V-B, we calculated the *k* parameter in several slices from the same dataset. The parameter *t* that represents the time in the anisotropic diffusion was experimentally established as 10 iterations.

For quantitative analyses, we calculated the Peak Signal-to-Noise Ratio (PSNR) and the Mean Square Error (MSE) for comparing the enhanced images with the original images. As for quality, the measured values of MSE should be small and
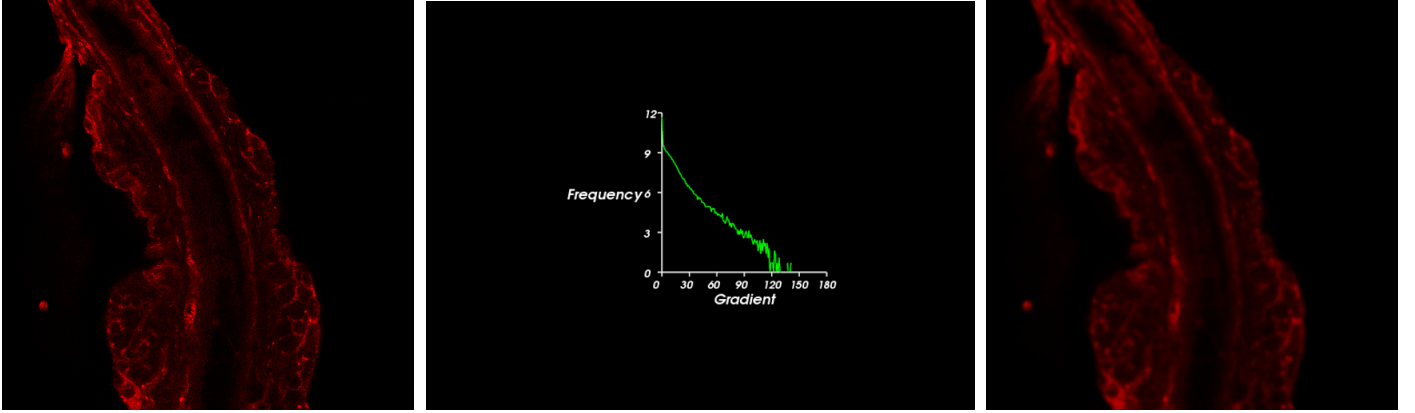
Fig. 3. Estimation of the k parameter using Perona and Malik's model. Left: Original slice. Center: Gradient histogram. Right: Anisotropic filtering result
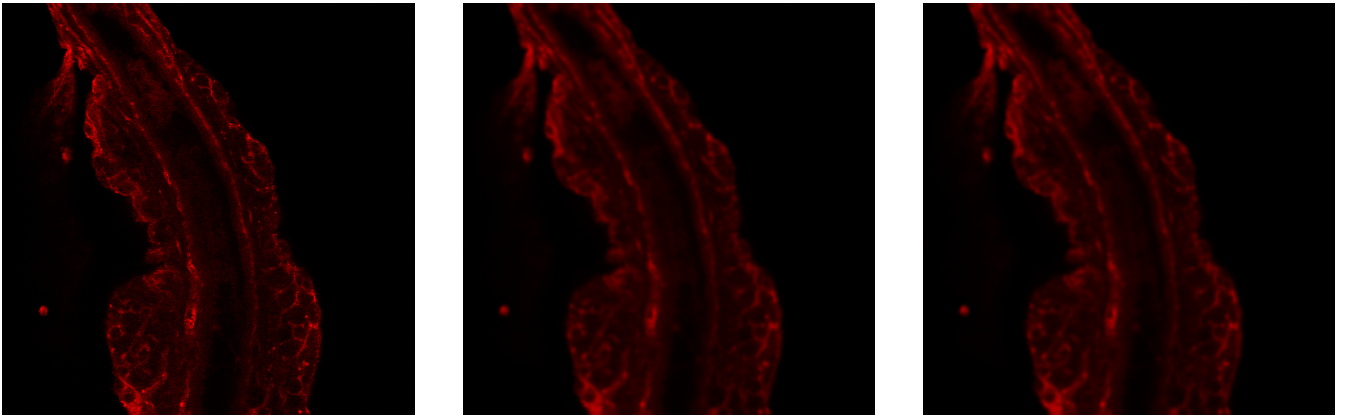

Fig. 4. Comparison of the anisotropic diffusion using the two models for estimating the k parameter. Left: Original slice. Center: Anisotropic filtering result using the Perona and Malik's model presented in Sec. V-A. Right: Anisotropic filtering result applying the Voci et al.'s model presented in Sec. V-B.

PSNR should be large. The PSNR and the MSE are defined by:

$$MSE = \frac{\sum_{i=1}^{r} \sum_{j=1}^{c} \mid I(i,j) - \hat{I}(i,j) \mid^2}{r.c} \quad (4)$$

where $I(i,j)$ is the original image, $\hat{I}(i,j)$ is the enhanced image, and $r.c$ the size of the image.

$$PSNR = 10 \log_{10}(\frac{MAX_I^2}{MSE}) \quad (5)$$

where $MAX_I = 2^n - 1$ and n is the number of bits. Since the confocal images are 8-bits depth, n is set to 255.

Table II and Table III show the k values and the respective measures of MSE and PSNR of the enhanced images.

After applying the anisotropic diffusion with both models, we verified that PSNR values are very similar in the resulting images. In terms of image quality this means that the two models are adequate for enhancing our images.

For enhancing the whole confocal dataset using the two models presented in Section V-A and Section V-B, we calculated the average value of k considering all slices. The results for the enhanced volume are shown in Fig. 5.

As for qualitative analyses, we invited a senior hepatologist to describe how he found the enhanced volume in comparison to the original volume. According to the hepatologist, the resulting volumetric visualization solves some problems

TABLE II
k PARAMETER ACCORDING TO PERONA AND MALIK'S MODEL AND MSE, PSNR OF THE ENHANCED IMAGES

| mouse2-day7	k parameter	MSE	PSNR
Slice #1	131	25.0112	34.1494
Slice #10	139	25.7968	34.0151
Slice #20	139	25.9635	33.9871
Slice #30	138	26.9295	33.8285
Slice #43	137	29.4593	33.4385
Slice #50	155	30.9956	33.2177
Slice #60	156	32.7181	32.9829
Slice #70	145	34.3088	32.7767
Slice #80	138	34.8454	32.7093
Slice # 90	144	35.4471	32.6349
Slice #100	155	34.242	32.7852
Slice #110	137	31.7267	33.1165
Slice #120	147	27.1433	33.7941
Slice #130	141	22.3949	34.6293
Slice #140	144	18.1274	35.5474
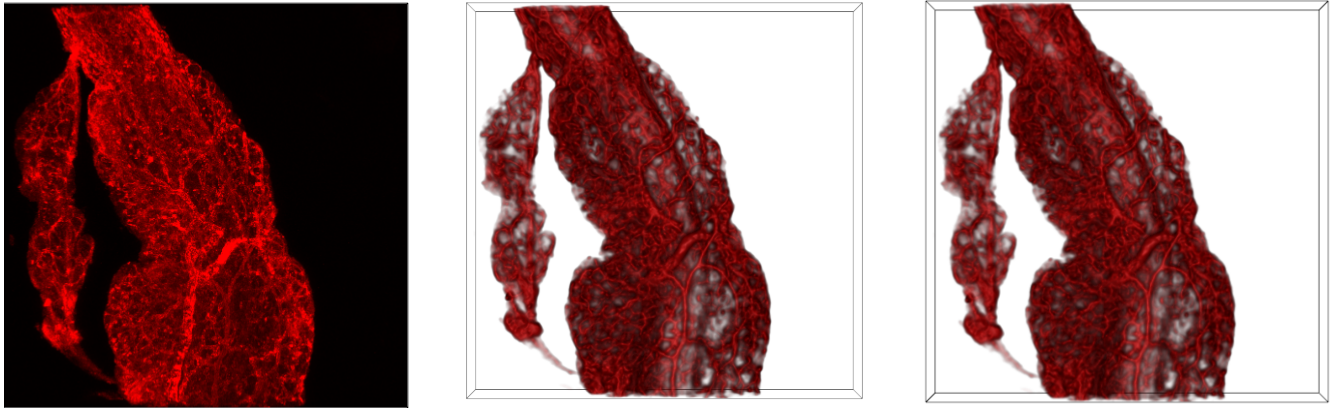
Fig. 5. Comparison of the anisotropic diffusion using the two models for estimating the k parameter. Left: Original reconstructed volume. Center: anisotropic filtering results using Perona and Malik's model. Right: anisotropic filtering results using Voci et al.'s model

TABLE III
k PARAMETER ACCORDING TO VOCI ET AL.'S MODEL AND MSE, PSNR
OF THE ENHANCED IMAGES

mouse2-day7	k parameter	MSE	PSNR
Slice #1	243	25.0208	34.1477
Slice #10	240	25.8104	34.0128
Slice #20	242	25.9736	33.9854
Slice #30	242	26.9542	33.8245
Slice #43	236	29.4543	33.4393
Slice #50	238	30.9819	33.2197
Slice #60	223	32.7058	32.9845
Slice #70	124	34.2854	32.7797
Slice #80	123	34.8371	32.7103
Slice # 90	123	35.4506	32.6345
Slice #100	126	34.2397	32.7854
Slice #110	139	31.7235	33.1169
Slice #120	140	27.1388	33.7948
Slice # 130	159	22.4014	34.628
Slice #140	182	18.141	35.5441

associated to the original data such as noise and superposition of vessels. He also commented that the microvasculature was clearly discernible, which gives a better idea of the 3D distribution of the vessels. This observation is really important because it represents that our method allows hepatologists to evaluate morphological alterations in the bile ducts.

VII. FINAL COMMENTS AND FUTURE WORK

The study of bile ducts and associated vessels is an important goal of current hepatology research. Microscopic visualization is essential to the analyses of the interrelationship between a bile duct and its vascular plexus. The acquired confocal images are affected by several sources of noise. So, the first step in the analyses of the microvasculature is to improve the quality of the acquired images.

In this paper, we presented experimental results of applying anisotropic diffusion to enhance noisy confocal images of bile ducts. We applied anisotropic diffusion in several slices and compared their image quality using quantitative measures such as PSNR and MSE. Qualitative analysis by an expert has shown that our results so far provide a better context for the visual study of bile ducts' microvasculature.

As for future work, there are several possibilities for helping the understanding of the development of biliary diseases associated with vascular disorders. We intend to give support for quantitative analysis such as measuring the size of the structures, as well as devising shape analysis methods tailored for the microvasculature study.

REFERENCES

[1] C. S. R. Babu and M. Sharma, "Biliary tract anatomy and its relationship with venous drainage," *Journal of clinical and experimental hepatology*, vol. 4, pp. S18–S26, 2014.

[2] A. Lametschwandtner, H. Bartel, C. Radner, and B. Minnich, "Histomorphology and microvasculature of extrahepatic bile ducts, extrapancreatic ducts and choledocho-pancreatic duct in the adult african clawed toad, xenopus laevis: Histomorphology and scanning electron microscopy of microvascular corrosion casts," *Transactions of the Royal Society of South Africa*, pp. 1–10, 2015.

[3] S. Hammad, S. Hoehme, A. Friebel, I. Von Recklinghausen, A. Othman, B. Begher-Tibbe, R. Reif, P. Godoy, T. Johann, A. Vartak *et al.*, "Protocols for staining of bile canalicular and sinusoidal networks of human, mouse and pig livers, three-dimensional reconstruction and quantification of tissue microarchitecture by image processing and analysis," *Archives of toxicology*, vol. 88, no. 5, pp. 1161–1183, 2014.

[4] N. Vartak, A. Damle-Vartak, B. Richter, O. Dirsch, U. Dahmen, S. Hammad, and J. G. Hengstler, "Cholestasis-induced adaptive remodeling of interlobular bile ducts," *Hepatology*, 2016.

[5] F. DiPaola, P. Shivakumar, J. Pfister, S. Walters, G. Sabla, and J. A. Bezerra, "Identification of intramural epithelial networks linked to peribiliary glands that express progenitor cell markers and proliferate after injury in mice," *Hepatology: Official Journal of the American Association for the Study of Liver Diseases*, 2013.

[6] Y.-Y. Fu, C.-W. Lin, G. Enikolopov, E. Sibley, A.-S. Chiang, and S.-C. Tang, "Microtome-free 3-dimensional confocal imaging method for visualization of mouse intestine with subcellular-level resolution," *Gastroenterology*, vol. 137, no. 2, pp. 453–465, 2009.

[7] Y.-C. Chen, Y.-C. Chen, and A.-S. Chiang, "Template-driven segmentation of confocal microscopy images," *Computer Methods and Programs in Biomedicine*, vol. 89, no. 3, pp. 239 – 247, 2008.

[8] N. Ramesh, H. Otsuna, and T. Tasdizen, "Three-dimensional alignment and merging of confocal microscopy stacks," in *2013 IEEE International Conference on Image Processing*, Sept 2013, pp. 1447–1450.

[9] J. Weickert, *Anisotropic diffusion in image processing*. Teubner Stuttgart, 1998, vol. 1.

[10] A. S. Frangakis and R. Hegerl, "Noise reduction in electron tomographic reconstructions using nonlinear anisotropic diffusion," *Journal of structural biology*, vol. 135, no. 3, pp. 239–250, 2001.

[11] G. Gavriloaia, C. Neamtu, M. Gavriloaia, and A. Ghemigan, "Anisotropic diffusion filtering of infrared medical images," in *Systems, Signals and Image Processing (IWSSIP), 2011 18th International Conference on*, June 2011, pp. 1–4.

[12] V. Ruela Pereira Borges, D. Junqueira dos Santos, B. Popovic, and D. Farias Cordeiro, "Segmentation of blood vessels in retinal images based on nonlinear filtering," in *Computer-Based Medical Systems (CBMS), 2015 IEEE 28th International Symposium on*. IEEE, 2015, pp. 95–96.

[13] K. Washington, P.-A. Clavien, and P. Killenberg, "Peribiliary vascular plexus in primary sclerosing cholangitis and primary biliary cirrhosis," *Human pathology*, vol. 28, no. 7, pp. 791–795, 1997.

[14] N. S. Claxton, T. J. Fellers, and M. W. Davidson, "Laser scanning confocal microscopy," *Department of Optical Microscopy and Digital Imaging, Florida State University, Tallahassee, http://www. olympusconfocal. com/theory/LSCMIntro. pdf*, 2006.

[15] Y. Wan, H. Otsuna, C.-B. Chien, and C. Hansen, "Fluorender: an application of 2d image space methods for 3d and 4d confocal microscopy data visualization in neurobiology research," in *Visualization Symposium (PacificVis), 2012 IEEE Pacific*. IEEE, 2012, pp. 201–208.

[16] Michael W. Davidson., "Basic concepts in fluorescence," http://micro.magnet.fsu.edu/primer/techniques/fluorescence/fluorescenceintro.html, June 2014, accessed on: November 2015.

[17] R. L. Price and W. G. Jerome, *Basic Confocal Microscopy*. New York: Springer, 2011.

[18] J. Toriwaki and H. Yoshida, *Fundamental of Three Dimensional Digital Image Processing*. New York: Springer, 2009.

[19] Y. Wan, H. Otsuna, C.-B. Chien, and C. Hansen, "An interactive visualization tool for multi-channel confocal microscopy data in neurobiology research," *Visualization and Computer Graphics, IEEE Transactions on*, vol. 15, no. 6, pp. 1489–1496, 2009.

[20] P. Perona and J. Malik, "Scale-space and edge detection using anisotropic diffusion," *Pattern Analysis and Machine Intelligence, IEEE Transactions on*, vol. 12, no. 7, pp. 629–639, 1990.

[21] L. Formaggia, A. Quarteroni, and A. Veneziani, *Cardiovascular Mathematics: Modeling and simulation of the circulatory system*. Springer Science & Business Media, 2010, vol. 1.

[22] C. Tsiotsios and M. Petrou, "On the choice of the parameters for anisotropic diffusion in image processing," *Pattern Recognition*, vol. 46, no. 5, pp. 1369 – 1381, 2013.

[23] J. Yuan and J. Wang, "Perona–malik model with a new diffusion coefficient for image denoising," *International Journal of Image and Graphics*, vol. 16, no. 02, p. 1650011, 2016.

[24] S. Inoué, "Microtubule dynamics in cell division: exploring living cells with polarized light microscopy," *Annual review of cell and developmental biology*, vol. 24, pp. 1–28, 2008.

[25] O. Rubel, G. H. Weber, M.-Y. Huang, E. W. Bethel, M. D. Biggin, C. C. Fowlkes, C. L. Luengo Hendriks, S. V. Keranen, M. B. Eisen, D. W. Knowles *et al.*, "Integrating data clustering and visualization for the analysis of 3d gene expression data," *Computational Biology and Bioinformatics, IEEE/ACM Transactions on*, vol. 7, no. 1, pp. 64–79, 2010.

[26] I. U. Rafalska-Metcalf and S. M. Janicki, "Show and tell: visualizing gene expression in living cells," *Journal of cell science*, vol. 120, no. 14, pp. 2301–2307, 2007.

[27] F. Long, H. Peng, X. Liu, S. K. Kim, and E. Myers, "A 3d digital atlas of c. elegans and its application to single-cell analyses," *Nature methods*, vol. 6, no. 9, pp. 667–672, 2009.

[28] H. Peng, Z. Ruan, D. Atasoy, and S. Sternson, "Automatic reconstruction of 3d neuron structures using a graph-augmented deformable model," *Bioinformatics*, vol. 26, no. 12, pp. i38–i46, 2010.

[29] H. Peng, F. Long, and G. Myers, "Automatic 3d neuron tracing using all-path pruning," *Bioinformatics*, vol. 27, no. 13, pp. i239–i247, 2011.

[30] E. Meijering, M. Jacob, J.-C. Sarria, P. Steiner, H. Hirling, and M. Unser, "Design and validation of a tool for neurite tracing and analysis in fluorescence microscopy images," *Cytometry Part A*, vol. 58, no. 2, pp. 167–176, 2004.

[31] F. Parazza, C. Humbert, and Y. Usson, "Method for 3d volumetric analysis of intranuclear fluorescence distribution in confocal microscopy," *Computerized medical imaging and graphics*, vol. 17, no. 3, pp. 189–200, 1993.

[32] M. Maddah, H. Soltanian-Zadeh, and A. Afzali-Kusha, "Snake modeling and distance transform approach to vascular centerline extraction and quantification," *Computerized Medical Imaging and Graphics*, vol. 27, no. 6, pp. 503–512, 2003.

[33] P. Paul, H. Duessmann, T. Bernas, H. Huber, and D. Kalamatianos, "Automatic noise quantification for confocal fluorescence microscopy images," *Computerized Medical Imaging and Graphics*, vol. 34, no. 6, pp. 426–434, 2010.

[34] A. D. A. Araujo, B. M. D. Faria, H. J. Rees, and M. A. R. Silva, "Enhancing microscope biological images with dip techniques," in *Computer Graphics and Image Processing, 2000. Proceedings XIII Brazilian Symposium on*, 2000, pp. 349–.

[35] F. Voci, S. Eiho, N. Sugimoto, and H. Sekibuchi, "Estimating the gradient in the perona-malik equation," *Signal Processing Magazine, IEEE*, vol. 21, no. 3, pp. 39–65, 2004.

[36] *The Visualization Toolkit User's Guide*, Kitware, Inc., January 2003.

[37] P. Kankaanpää, L. Paavolainen, S. Tiitta, M. Karjalainen, J. Päivärinne, J. Nieminen, V. Marjomäki, J. Heino, and D. J. White, "Bioimagexd: an open, general-purpose and high-throughput image-processing platform," *Nature methods*, vol. 9, no. 7, pp. 683–689, 2012.

[38] N. Díaz Rodríguez, P. Kankaanpää, M. M. Saleemi, J. Lilius, and I. Porres, "Programming biomedical smart space applications with bioimagexd and pythonrules," in *4th International Workshop on Semantic Web Applications and Tools for the Life Sciences (SWAT4LS 2011)*, A. Paschke, A. Burger, P. Romano, M. S. Marshall, and A. Splendiani, Eds. ACM, 2011, p. 10–11.